Mechanical Systems and Signal Processing 159 (2021) 107808

Contents lists available at ScienceDirect

Mechanical Systems and Signal Processing

journal homepage: www.elsevier.com/locate/ymssp

Continuous contact force model with an arbitrary damping term exponent: Model and discussion

Jie Zhang [a], CanHuang [a], Lei Zhao [a], JiejianDi [a], Guangping He [a], Wenhao Li [b,c,*]

[a] School of Mechanical and Materials Engineering, North China University of Technology, No. 9, Jinyuanzhuang Road, Shijingshan District, Beijing 100144, China
[b] Institute of Mechanics, Chinese Academy of Sciences, No. 15 Beisihuanxi Road, Haidian District, Beijing 100190, China
[c] School of Engineering Science, University of Chinese Academy of Sciences, No. 19(A) Yuquan Road, Shijingshan District, Beijing 100049, China

ARTICLE INFO

Article history:
Received 20 August 2020
Received in revised form 31 January 2021
Accepted 28 February 2021
Available online 19 March 2021
Communicated by John E. Mottershead

Keywords:
Contact model
Impact
Damping term exponent
Approximate dynamic equation

ABSTRACT

More than twenty continuous contact force models have been presented for modeling contact-impact problems; however, there was no uniformity regarding the value of the damping term exponent in these models. A new type of continuous contact force model is proposed in this research, in which the value of the damping term exponent can be arbitrary. Then, the effect of the value of the damping term exponent on the model accuracy is investigated by comparing the simulation and experimental results. As it is almost impossible to obtain an analytical solution based on the system dynamic equation, according to the rule of energy equivalence, an approximate dynamic equation is developed by introducing an equivalent indentation and equivalent velocity. Based on the system dynamic equation and the approximate dynamic equation, a primary formula for the hysteresis damping factor of the model can be obtained. Through nondimensional analysis, new models for different values of the damping term exponent are established by modifying the primary formula. The comparison between the simulation results and published experimental data demonstrates the validities of the new models and reveals that the influence of the value of the damping term exponent on the model accuracy can be considered to be negligible.

1. Introduction

Contact-impact phenomena are commonly found in nature and frequently occur in mechanical systems, with a short duration, a large collision force, fast energy dissipation and severe velocity changes [1]. Proper modeling of contact-impact phenomena is very important for an accurate description of the system dynamics behavior and has attracted much attention from researchers [2–6].

Newton introduced the concept of the coefficient of restitution in terms of the change in velocity, which provided a concise description of the impact phenomenon. Since then, scientists have defined the coefficient of restitution in terms of impulse and energy, and Newton's definition is the most commonly used definition [7]. The restitution coefficient is easy to experimentally determine [8], but it is not possible to provide details of the impact phenomenon, such as the contact force and deformation. For rigid body systems, researchers have proposed a nonsmooth method for calculating the contact force, which includes two main methods: the linear complementarity problem (LCP) [9,10] and differential variational inequality

* Corresponding author at: No.15 Beisihuanxi Road, Haidian District, Beijing 100190, China.
E-mail address: liwenhao@imech.ac.cn (W. Li).

https://doi.org/10.1016/j.ymssp.2021.107808
0888-3270/

Nomenclature

i, j	impactor, target
$v_i^{(-)}$, $v_j^{(-)}$	initial velocity
$v_i^{(+)}$, $v_j^{(+)}$	separation velocity
$t^{(-)}$, $t^{(+)}$,tm	time of initial contact, time of separation, time of maximum indentation
δ, δ_{max}	deformation or indentation, maximum indentation
v_{ij}	velocity of the objects at timetm
$\dot{\delta}$, $\ddot{\delta}$	deformation velocity or indentation velocity, indentation acceleration
m0, k	equivalent mass, equivalent stiffness
F_c, F_{max}	normal contact force, peak contact force
n	elastic term exponent
m	damping term exponent
cr	coefficient of restitution
λ	hysteresis damping factor
$\dot{\delta}^{(-)}$, $\dot{\delta}^{(+)}$	initial indentation velocity, relative separation velocity
$\widehat{\delta}$	equivalent indentation depth
$\widehat{\dot{\delta}}$, $\widehat{\dot{\delta}}_c$,$\widehat{\dot{\delta}}_r$	equivalent velocity, equivalent velocity of compression phase, equivalent velocity of restitution phase
T, t_c,t_r	time of the whole contact phase, compression phase and restitution phase
ΔE_{loss}	energy loss
ΔE_c, ΔE_r	energy loss for compression or restitution phase calculating based on the system dynamic equation
ΔE_c^*, ΔE_r^*	energy loss for compression or restitution phase calculating based on the approximate dynamic equation
ΔE_k	elastic potential energy
x, τ	non-dimensional variables
$\dot{x}$	derivative of x with respect toτ
$\dot{x}^{(-)}$, $\dot{x}^{(+)}$	initial and final values of$\dot{x}$
α	modification parameter
k^*, λ^*	non-dimensional parameters

(DVI) [11,12]. The nonsmooth method assumes that the impact is completed instantaneously and is not valid for modeling the contact process [13–16]. The algorithms for dealing with contact-impact problems in the finite element method and the boundary element method can model the contact process and calculate the contact forces and deformations, such as penalty method and Lagrange multiplier approach. However, these algorithms in the finite element method and the boundary element method are computationally intensive and not suitable for real-time analysis [17].

The compliant continuous contact force models can simulate the contact-impact process with high computational efficiency, and the contact forces of these models are modeled as continuous functions of the indentation depth and deformation velocity [5]. In 1880, Hertz proposed the Hertz contact model [18], which no longer treated the contact behavior as instantaneous but as an ongoing process, and the contact force was defined as a function of the indentation depth δ: $F_c = k\delta^n$, where k represents the generalized stiffness parameter and the exponent n depends on the topological properties of the contacting surfaces [19]. The Hertz model depicts the local deformation of the contacting bodies in terms of the indentation depth, which is caused by deformation. The duration time and time histories of the velocity, contact force and indentation depth δ can be described by this model. The Hertz model is still an important part of contact mechanics and is widely used in many fields, especially for quasi-static contact problems. However, this model cannot take into account the energy dissipation during a collision [7].

Energy dissipation inevitably exists during the impact process. The Kelvin-Voigt model simulates the energy dissipation by introducing a damping term, and the contact force is modeled as $F_c = k\delta + \lambda\dot{\delta}$, where $\dot{\delta}$ is the deformation velocity and λ is the hysteresis damping factor. However, the contact force calculated by this model is nonzero when the deformation is zero, which goes against the physical behavior [7], and the accuracy of this model is relatively low.

Hunt and Crossley [20] proposed a contact model based on the Hertz model that can take into account the energy dissipation. In this model, the contact force is composed of an elastic force and a dissipative force, which is described as $F_c = k\delta^n + \lambda\delta^n\dot{\delta}$. When the deformation is zero, the contact force equals zero; when the deformation velocity $\dot{\delta}$ approaches zero, the contact condition becomes quasi-static. Due to the nonlinear coupling between the indentation δ and deformation velocity $\dot{\delta}$ in the damping term $\lambda\delta^n\dot{\delta}$, the analytical solution of the system dynamic equation constructed based on this contact force model is difficult to obtained [7]. In recent years, more than ten continuous contact models have been proposed based on the work of Hunt and Crossley [14,20,21–28], and several continuous contact models have been proposed with contact forces in a form that is similar to that of the Hunt and Crossley model [29–37]. The determination of the expression of λ becomes the crucial step in the construction of this kind of model [19]. These models are divided into two categories based on the expression of λ: the preimpact velocity-dependent model and the preimpact velocity-independent model [5].

The applications for this kind of model include simulations of robotics [2], vehicles, sand [38], clay, seeds [39], hail specimens [40], structural pounding during earthquakes [41], aero-engines [42] and the contact process between the barrel and bourrelet of the projectile [43]. Its application has also been extended to the simulation of the discrete element method [44] and smoothed particle hydrodynamics [5].

Table 1 summarizes the published continuous contact force models. A general expression for the contact force can be described as $F_c = k\delta^n + \lambda\delta^m\dot{\delta}$, where m is the damping term exponent [13]. In the research of Hunt and Crossley, m is assumed to be equal to n without a theoretical basis [20]. It can be seen that in some studies, the value of m is not equal to the value of n, and its value has been set to 1.0 [29–31], 0.65 [32], 0.5 [33–36] and 0.25 [37] when n equals 1.5. This naturally raises the following questions: How much does the value of the damping term exponent m affect the accuracy of the continuous contact force model? Whether there is an optimal value of m for the continuous contact force model that can provide the best model accuracy for the description of contact-impact phenomena requires investigation.

Previous studies on the continuous contact force model have focused on the establishment of the damping coefficient λ and the application of the models [5], but few studies addressed the effect of the m-values on the model accuracy. A method for estimating damping parameters (λ and m) has been proposed based on the experimental measurements and analytical calculations of a cam-follower system [45], the optimum values of damping parameters are m = 1.55 and $\lambda = 92.6\mathrm{GN}sm^{-2.55}$. However, the chief limitation of this research is the indirect estimation of damping parameters [45], the damping coefficient λ is determined on the basis of experimental results rather than on the basis of the formula of continuous contact force models. Therefore, the conclusion of [45] cannot be directly applied to the parameters determination of the continuous contact force models. It may also be noted that for the case when $n \neq m$ and n is arbitrary (which means that the contacting object surface has a complex geometry [46]), no corresponding continuous contact force model has been proposed.

To address this issue, this work develops a new type of continuous contact force model with an arbitrary damping term exponent m, and the effect of the value of m on the accuracy of the continuous contact force models is discussed. As there is no analytical solution of the system dynamic equation, an approximate dynamic equation is presented in Section 2.2 by introducing equivalent indentation and equivalent velocity, and a primary formula for the hysteresis damping factor λ is derived in Section 2.3. In Section 2.4, the deviation between the approximate dynamic equation and the system dynamic equation is investigated by numerical examples. The new models for different values of m are developed in Section 2.5 by modifying the primary formula of λ through nondimensional analysis. The comparison between the simulation results and published experimental data is conducted in Section 3, which demonstrates the validity of the new models and reveals the effect of the value of the damping term exponent on the model accuracy.

2. The development of the new model

2.1. General issues regarding the construction of the new model

As shown in Fig. 1a, the general situation of the direct central normal impact between two objects (with masses m_i and m_j) is considered, and the entire impact process is divided into two phases: the compression phase and the restitution phase [7]. At the initial time of impact $t^{(-)}$, the objects have velocities $v_i^{(-)}$ and $v_j^{(-)}$. Then, the deformation will increase in the local zone, as the contacting bodies reach the same velocity v_{ij}, the relative normal deformation δ reaches a maximum δ_{max} at time t_m, and the period from $t^{(-)}$ to t_m is the compression phase. After that, the deformation begins to recover, the contact force gradually decreases until it becomes zero at time $t^{(+)}$, and the velocities become $v_i^{(+)}$ and $v_j^{(+)}$. The period from tm to $t^{(+)}$ is the restitution phase. When the sizes of the contacting objects are much larger than the size of the contact area, the contact-impact system with two objects can be equivalent to an impact between an elastic half space and an object with equivalent mass $m_0 = \frac{m_i m_j}{m_i+m_j}$ and equivalent initial velocity $\dot{\delta}^{(-)} = v_i^{(-)} - v_j^{(-)}$ [26,47], as illustrated in Fig. 1b. This equivalence can be applied to most elastic contact-impact problems [45,47].

The general expression for the contact force of the compliant continuous contact force model is described below [13]:

$$F_c = k\delta^n + \lambda\delta^m\dot{\delta} \tag{1}$$

Table 1
Summarize of the continuous contact force models.

Expression of the contact force		Value of the elastic term exponent n	Value of the damping term exponent m
$F_c = k\delta^n$		arbitrary n	m = 0
$F_c = k\delta + \lambda\dot{\delta}$	$m = n$	n = 1	m = 1
$F_c = k\delta^n + \lambda\delta^m\dot{\delta}$	$m = n$	n = 1.5	m = 1.5 [7,26–28]
		arbitrary n	$m = n$ [14,19–24,32]
	$m \neq n$	n = 1.5	m = 1.0 [29–31]; m = 0.65 [32]; m = 0.5 [33–36]; m = 0.25 [37];
		arbitrary n	null

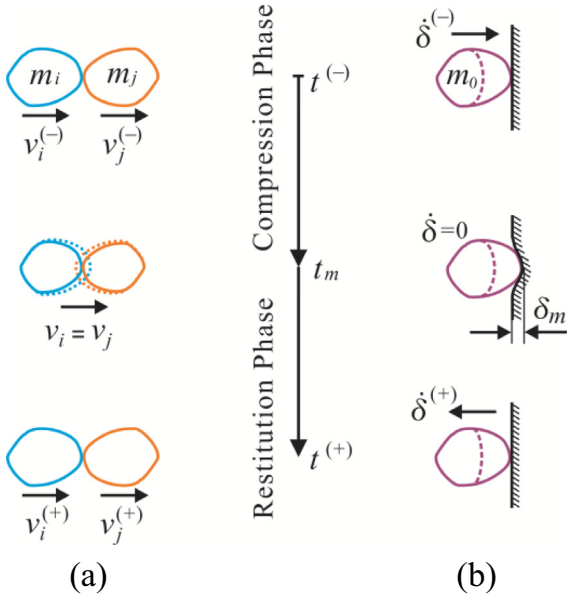

Fig. 1. Direct central collision: (a) Contact-impact system with two objects; (b) The equivalent system.

When two spheres are in contact, the exponent n equals 1.5, and the expression of stiffness parameter k, which is dependent on the material properties and the topological properties of the contacting surfaces, is as follows [7,26]:

$$k = \frac{4E^*}{3}\left[\frac{r_i r_j}{r_i + r_j}\right]^{\frac{1}{2}} \tag{2}$$

where r_i and r_j are the radius of spheres, the material parameter E^* is

$$\frac{1}{E^*} = \frac{1-\tau_1^2}{E_1} + \frac{1-\tau_2^2}{E_2} \tag{3}$$

where τ_i and E_i are the Poisson's ratio and Young's modulus associated with each sphere, respectively.

Besides the contact between two spheres, theoretical analysis shows that for the contact between a cube, prism, cylinder (horizontal and vertical), or cone and an elastic half space, the n value is 1.0, 1.0, 1.0, 1.0 or 2.0, respectively, in other situations the n value can be obtained numerically [19]. More details about the determination of the values of k and n for different contact-impact problems can be found in relevant literature [46].

In Eq. (1), $k\delta^n$ is the elastic force and $\lambda\delta^m\dot{\delta}$ is the dissipative damping force. The dynamic equation for the contact-impact systems as shown in Fig. 1 can be described as,

$$m_0\ddot{\delta} + k\delta^n + \lambda\delta^m\dot{\delta} = 0 \tag{4}$$

where the equivalent mass $m_0 = \frac{m_i m_j}{m_i + m_j}$.

The crucial step in the construction of this kind of contact model is the determination of the expression of λ [19]. Due to the nonlinear coupling term $\delta^m\dot{\delta}$ in the contact force expression, it is almost impossible to obtain an analytical solution of λ based on the system dynamic Eq. (4) [19]. In previous studies, the simpler equations than Eq. (4), such as $m_0\ddot{\delta} + k\delta^n = 0$[26] and [7,40]$m_0\ddot{\delta} + k\delta + \lambda\dot{\delta} = 0$, were used to construct a functional relationship between the deformation velocity and indentation, and then combined with Eq. (4), the expressions for λ can be obtained. Jie Zhang et al have been proposed a new contact force model based on approximate dynamic equation $m_0\ddot{\delta} + k\delta^n + \lambda\hat{\dot{\delta}}\delta^n = 0$ and the damping factor λ was more rigorously derived. Simulation results had shown high accuracy of the correlation models [7,19,26]. However, in these studies the damping term exponent m is assumed to be equal to the elastic term n without a theoretical basis [20]. Inspired by the previous works [7,19,26], a new continuous contact force model is proposed in this research, in which the value of the damping term exponent m can be arbitrary.

2.2. Approximate dynamic equation for the impact system

Based on the rule of energy equivalence, an approximate dynamic equation is developed in this section, which achieves a good approximation of the system dynamic equation and can be an important basis for the derivation of λ.

The system dynamic equation shown in Eq. (4) can be revised as follows

$$m_0\ddot{\delta} + \left(k\delta^{n-m} + \lambda\dot{\delta}\right)\delta^m = 0 \tag{5}$$

Consider first an approximate dynamic equation similar to Eq. (5):

$$m_0\ddot{\delta} + \left(\widehat{\delta}^{n-m} + \widehat{\lambda}\widehat{\dot{\delta}}\right)k\delta^m = 0 \tag{6}$$

where $\widehat{\lambda} = \frac{\lambda}{k}$, $\widehat{\delta}$ is the equivalent indentation, which is a constant and associated with δ_{max}, $\widehat{\dot{\delta}}$ is the equivalent velocity associated with $\dot{\delta}^{(-)}$, and remains unchanged during the compression and restitution phases [19]. The corresponding approximate contact force can be expressed as

$$F_c = k\left(\widehat{\delta}^{n-m} + \widehat{\lambda}\widehat{\dot{\delta}}\right)\delta^m = k\widehat{\delta}^{n-m}\delta^m + \lambda\widehat{\dot{\delta}}\delta^m \tag{7}$$

Eq. (7) is an approximate form of Eq. (1), where $k\widehat{\delta}^{n-m}\delta^m$ and $\lambda\widehat{\dot{\delta}}\delta^m$ correspond to the elastic force term $k\delta^n$ and damping force term $\lambda\delta^m\dot{\delta}$ of Eq. (1), respectively. More details will be discussed in the following.

Eq. (6) can be expressed as

$$m_0\frac{d\dot{\delta}}{dt} + \left(\widehat{\delta}^{n-m} + \widehat{\lambda}\widehat{\dot{\delta}}\right)k\delta^m = m_0\frac{d\dot{\delta}}{d\delta}\frac{d\delta}{dt} + \left(\widehat{\delta}^{n-m} + \widehat{\lambda}\widehat{\dot{\delta}}\right)k\delta^m = 0 \tag{8}$$

Then it can be revised as

$$m_0\dot{\delta}\mathrm{d}\dot{\delta} = -\left(\widehat{\delta}^{n-m} + \widehat{\lambda}\widehat{\dot{\delta}}\right)k\delta^m d\delta \tag{9}$$

Integrating Eq. (9) over the compression phase, it can be deduced that,

$$\dot{\delta}^2 - \dot{\delta}^{(-)2} = -\frac{2k\left(\widehat{\delta}^{n-m} + \widehat{\lambda}\widehat{\dot{\delta}}_c\right)}{m_0(m+1)}\delta^{m+1} \tag{10}$$

where $\widehat{\dot{\delta}}_c$ is the equivalent velocity of the compression phase. As the deformation velocity $\dot{\delta} = 0$, the indentation depth δ reaches its maximum value, which can be obtained by substituting $\dot{\delta} = 0$ into Eq. (10):

$$\delta_{max}^{m+1} = \frac{m_0(m+1)}{2k\left(\widehat{\delta}^{n-m} + \widehat{\lambda}\widehat{\dot{\delta}}_c\right)}\dot{\delta}^{(-)2} \tag{11}$$

The relationship between deformation velocity $\dot{\delta}$ and indentation depth δ during the compression phase can be obtained from Eqs. (10) and (11),

$$\dot{\delta} = \dot{\delta}^{(-)}\sqrt{1 - \left(\frac{\delta}{\delta_{max}}\right)^{m+1}} \tag{12}$$

Then the work done by the damping force and elastic force in Eqs. (1) and (7) can be calculated, respectively. And based on the rule of energy equivalence, the equivalent indentation $\widehat{\delta}$ and the equivalent velocity $\widehat{\dot{\delta}}$ of the approximate dynamic equation can be derived.

Firstly, the work done by the dissipative force in the compression phase can be calculated based on the system dynamic Eqs. (4) and (12), it should be noted that Eq. (12) is derived from the approximate dynamic equation,

$$\Delta E_c = \int_0^{\delta_{max}} \lambda\delta^m\dot{\delta}d\delta = \int_0^{\delta_{max}} \lambda\delta^m\dot{\delta}^{(-)}\sqrt{1 - \left(\frac{\delta}{\delta_{max}}\right)^{m+1}}d\delta \tag{13}$$

$$= \int_0^1 \frac{\lambda\delta_{max}^{m+1}\dot{\delta}^{(-)}}{m+1}\sqrt{1 - \left(\frac{\delta}{\delta_{max}}\right)^{m+1}}d\left(\frac{\delta}{\delta_{max}}\right)^{m+1}$$

$$= \int_0^1 \frac{\lambda\delta_{max}^{m+1}\dot{\delta}^{(-)}}{m+1}\sqrt{1-x}dx = \frac{\lambda\delta_{max}^{m+1}}{m+1}\cdot\frac{2\dot{\delta}^{(-)}}{3}$$

In addition, the work done by the dissipative force in the compression phase can be calculated based on the approximate dynamic Eq. (6), as follows

$$\Delta E_c^* = \int_0^{\delta_{max}} k\delta^m\widehat{\lambda}\widehat{\dot{\delta}}_c d\delta = \int_0^{\delta_{max}} \lambda\delta^m\widehat{\dot{\delta}}_c d\delta = \frac{\lambda\delta_{max}^{m+1}}{m+1}\widehat{\dot{\delta}}_c \tag{14}$$

Thus, the work done by the dissipative forces in the compression phase can be obtained based on the system dynamic equation and the approximate dynamic equation, respectively. Then based on the rule of energy equivalence, the equivalent velocity in the compression phase can be derived from Eqs. (13) and (14),

$$\hat{\dot{\delta}}_c = \frac{2\dot{\delta}^{(-)}}{3} \tag{15}$$

On the other hand, the work done by the elastic force in the compression phase can be obtained based on the system dynamic Eq. (4),

$$\int_0^{\delta_{max}} k\delta^m \delta^{n-m} d\delta = \int_0^{\delta_{max}} k\delta^n d\delta = \frac{k\delta_{max}^{n+1}}{n+1} \tag{16}$$

And the work done by the elastic force according to the approximate dynamic Eq. (6) is

$$\int_0^{\delta_{max}} k\delta^m \hat{\delta}^{n-m} d\delta = \frac{k\delta_{max}^{m+1}\hat{\delta}^{n-m}}{m+1} \tag{17}$$

Thus, based on the rule of energy equivalence, the equivalent indentation $\hat{\delta}$ can be derived

$$\hat{\delta}^{n-m} = \frac{m+1}{n+1}\delta_{max}^{n-m} \tag{18}$$

Then let's consider the restitution phase. Similarly, the equivalent indentation and the equivalent velocity of the restitution phase can be deduced. Integrating Eq. (9) over the restitution phase, we obtain

$$\left(c_r\dot{\delta}^{(-)}\right)^2 - \dot{\delta}^2 = \frac{2k\left(\hat{\delta}^{n-m} + \hat{\lambda}\hat{\dot{\delta}}_r\right)}{m_0(m+1)}\delta^{m+1} \tag{19}$$

where $\hat{\dot{\delta}}_r$ is the equivalent velocity of the restitution phase. Substituting $\dot{\delta} = 0$ into Eq. (19) yields

$$\delta_{max}^{m+1} = \frac{m_0(n+1)}{2k\left(\hat{\delta}^{n-m} + \hat{\lambda}\hat{\dot{\delta}}_r\right)}\left(c_r\dot{\delta}^{(-)}\right)^2 \tag{20}$$

Since the velocities are in opposite directions in the restitution and compression phases, the relationship between deformation velocity $\dot{\delta}$ and indentation depth δ during the restitution phase can be derived from Eqs. (19) and (20):

$$\dot{\delta} = -c_r\dot{\delta}^{(-)}\sqrt{1 - \left(\frac{\delta}{\delta_{max}}\right)^{m+1}} \tag{21}$$

Then the work done by the dissipative force in the restitution phase can be obtained based on the system dynamic Eqs. (4) and (21), it should be noted that Eq. (21) is derived from the approximate dynamic equation,

$$\Delta E_r = \int_{\delta_{max}}^0 \lambda\delta^m\dot{\delta}d\delta = -\int_{\delta_{max}}^0 \lambda\delta^m c_r\dot{\delta}^{(-)}\sqrt{1 - \left(\frac{\delta}{\delta_{max}}\right)^{m+1}}d\delta = \frac{\lambda\delta_{max}^{m+1}}{m+1}\cdot\frac{2c_r\dot{\delta}^{(-)}}{3} \tag{22}$$

In addition, the work done by the dissipative force in the restitution phase can be calculated based on the approximate dynamic Eq. (6):

$$\Delta E_r^* = \int_{\delta_{max}}^0 k\delta^m\hat{\lambda}\hat{\dot{\delta}}_r d\delta = \int_{\delta_{max}}^0 \lambda\delta^m\hat{\dot{\delta}}_r d\delta = -\frac{\lambda\delta_{max}^{m+1}}{m+1}\hat{\dot{\delta}}_r \tag{23}$$

Then based on the rule of energy equivalence, the equivalent velocity in the restitution phase can be derived from Eqs. (22) and (23).

$$\hat{\dot{\delta}}_r = \frac{-2c_r\dot{\delta}^{(-)}}{3} \tag{24}$$

On the other hand, the work done by the elastic force in the restitution phase can be obtained based on the system dynamic Eq. (4),

$$\int_{\delta_{max}}^0 k\delta^n d\delta = -\frac{k\delta_{max}^{n+1}}{n+1} \tag{25}$$

And the work done by the elastic force according to the approximate dynamic Eq. (6) is

$$\int_{\delta_{max}}^{0} k\delta^m \widehat{\delta}^{n-m} d\delta = -\frac{k\delta_{max}^{m+1}\widehat{\delta}^{n-m}}{m+1} \tag{26}$$

Thus, the equivalent indentation can be derived based on the rule of energy equivalence, which is the same as Eq. (18),

$$\widehat{\delta}^{n-m} = \frac{m+1}{n+1}\delta_{max}^{n-m} \tag{27}$$

As described above, based on the rule of energy equivalence, the equivalent velocities $\widehat{\dot{\delta}}_c$, $\widehat{\dot{\delta}}_r$ and the equivalent indentation $\widehat{\delta}$ can be calculated, thus the approximate dynamic equation can be obtained by substituting Eqs. (15), (18), (24) and (27) into Eq. (6):

$$\begin{cases} m_0\ddot{\delta} + \left(\frac{m+1}{n+1}\delta_{max}^{n-m} + \widehat{\lambda}\frac{2\dot{\delta}^{(-)}}{3}\right)k\delta^m = 0 \text{Compression phase} \\ m_0\ddot{\delta} + \left(\frac{m+1}{n+1}\delta_{max}^{n-m} - \widehat{\lambda}\frac{2c_r\dot{\delta}^{(-)}}{3}\right)k\delta^m = 0 \text{Restitution phase} \end{cases} \tag{28}$$

The corresponding approximate contact force equation can be obtained by substituting Eqs. (15), (18), (24) and (27) into Eq. (7):

$$F_c = \begin{cases} k\left(\frac{m+1}{n+1}\delta_{max}^{n-m} + \widehat{\lambda}\frac{2\dot{\delta}^{(-)}}{3}\right)\delta^m = 0 \text{Compression phase} \\ k\left(\frac{m+1}{n+1}\delta_{max}^{n-m} - \widehat{\lambda}\frac{2c_r\dot{\delta}^{(-)}}{3}\right)\delta^m = 0 \text{Restitution phase} \end{cases} \tag{29}$$

Therefore, the expressions for approximate dynamic equation and approximate contact force equation are determined based on the rule of energy equivalence. From Eqs. (28) and (29) it can be seen that the approximate dynamic equation and the corresponding approximate contact force equation are in the form of piecewise functions and no longer contain the nonlinear coupling term $\delta^m\dot{\delta}$ as described in Eqs. (1) and (4). In terms of physical meaning, the approximate form of continuous model has an elastic term but no damping term, as illustrated in Fig. 2 and Eq. (29). Due to the initial velocity $\dot{\delta}^{(-)}$ is set to greater than zero, the stiffness coefficient in the compression phase is larger than that in the restitution phase. In general, it can be deduced from Eq. (29) that the contact forces in the compression phase are larger than that in the restitution phase. Thus, the magnitude of separating velocity $\dot{\delta}^{(+)}$ is smaller than the magnitude of initial velocity $\dot{\delta}^{(-)}$, which represents the onset of energy dissipation. From the above analysis, the approximate contact force equation and the approximate dynamic equation shown in Eqs. (28) and (29) simulate the energy dissipation by setting different stiffness coefficients in the compression phase and restitution phase. As shown in Fig. 2, the approximate contact force equation adopts the form of "Rigid spring in compression phase + Soft spring in restitution phase" to simulate energy dissipation, which avoids the nonlinear damping term in the continuous model. The approximate contact force equation is similar to Hertz model, except for the differences in stiffness coefficient.

The comparisons between compliant continuous contact force model and approximate contact force equation are illustrated in Table 2. It can be seen that the approximate contact force equation avoids the nonlinear coupling between the deformation velocity and indentation depth in the damping term, therefore the relationship between deformation velocity $\dot{\delta}$ and indentation depth δ can be deduced based on the approximate dynamic equation. This is a major advantage of the approximate contact force equation and approximate dynamic equation. As it is almost impossible to obtain an analytical solution of $\dot{\delta}(\delta)$ based on compliant continuous contact force model and system dynamic equation.

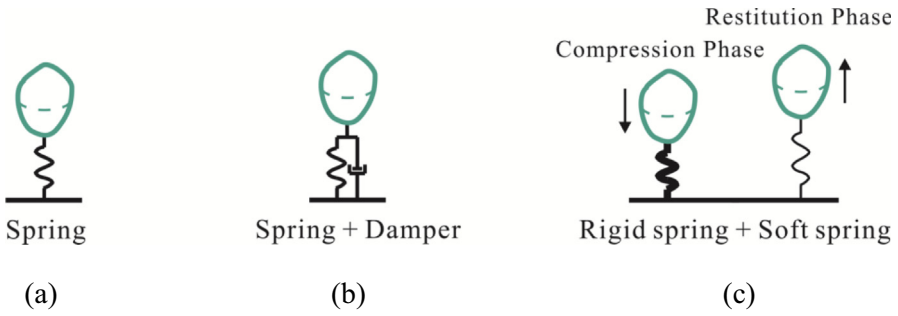

Fig. 2. Schematic diagram of compliant continuous contact force models: (a) Hertz model; (b) Compliant continuous contact model; (c) Approximate contact force equation.

Table 2
Comparisons between compliant continuous contact force model and approximate contact force equation.

	Compliant continuous contact force model	Approximate contact force equation
Expression of contact force	$F_c = k\delta^n + \lambda\delta^m\dot{\delta}$	$F_c = k\widehat{\delta}^{n-m}\delta^m + \lambda\widehat{\dot{\delta}}\delta^m$
Elastic force	$k\delta^n$	$k\widehat{\delta}^{n-m}\delta^m$
Dissipative force	$\lambda\dot{\delta}\delta^m$	$\lambda\widehat{\dot{\delta}}\delta^m$
Dynamic equation	$m_0\ddot{\delta} + k\delta^n + \lambda\delta^m\dot{\delta} = 0$	$m_0\ddot{\delta} + \left(\widehat{\delta}^{n-m} + \widehat{\lambda}\widehat{\dot{\delta}}\right)k\delta^m = 0$
$\dot{\delta}(\delta)$	Analytical solution has not been found	$\dot{\delta} = \dot{\delta}^{(-)}\sqrt{1-\left(\frac{\delta}{\delta_{max}}\right)^{m+1}}$

2.3. The primary formula of the hysteresis damping factor

The primary formula of the hysteresis damping factor λ can be obtained based on the system dynamic equation and the function $\dot{\delta}(\delta)$ which is derived from the approximate dynamic equation.

Firstly, according to the law of conservation of linear momentum and energy balance, the total energy loss ΔE_{loss} can be expressed in terms of the coefficient of restitution c_r [48],

$$\Delta E_{loss} = \frac{1}{2}m_0\left(1-c_r^2\right)\dot{\delta}^{(-)^2} \tag{30}$$

Based on Eqs. (13) and (22), we can obtain

$$\frac{\Delta E_c}{\Delta E_r} = \frac{1}{c_r} \tag{31}$$

It can be noted that the derivation of Eqs. (13) and (22) is based on the system dynamic equation and the function $\dot{\delta}(\delta)$ which is derived from the approximate dynamic equation.

Due to $\Delta E_{loss} = \Delta E_c + \Delta E_r$, substituting Eq. (31) into Eq. (30), it can be deduced that

$$\Delta E_c = \frac{m_0\dot{\delta}^{(-)^2}(1-c_r)}{2} \tag{32}$$

The elastic potential energy ΔE_k stored from $t^{(-)}$ to t_m can be derived based on the system dynamic equation,

$$\Delta E_k = \int_0^{\delta_{max}} k\delta^n d\delta = \frac{k\delta_{max}^{n+1}}{n+1} \tag{33}$$

According to the energy balance to the period from $t^{(-)}$ to t_m, we can obtain:

$$\frac{m_0\dot{\delta}^{(-)^2}}{2} = \frac{k\delta_{max}^{n+1}}{n+1} + \frac{m_0\dot{\delta}^{(-)^2}(1-c_r)}{2} \tag{34}$$

Then the maximum indentation can be deduced,

$$\delta_{max}^{n+1} = \frac{c_r m_0(n+1)\dot{\delta}^{(-)^2}}{2k} \tag{35}$$

Combining Eqs. (13), (32) and (35), the description of the hysteresis damping factor can be deduced,

$$\lambda = \frac{3m_0(m+1)(1-c_r)\dot{\delta}^{(-)}}{4}\left(\frac{c_r m_0(n+1)\dot{\delta}^{(-)^2}}{2k}\right)^{-\frac{m+1}{n+1}} \tag{36}$$

Therefore, an analytical solution for the hysteresis damping factor λ is obtained based on the system dynamic equation and the function $\dot{\delta}(\delta)$ which is derived from the approximate dynamic equation.

Similarly, combining Eqs. (14), (32) and (35), the description of the hysteresis damping factor with respect to the equivalent velocity $\widehat{\dot{\delta}}_c$ can be deduced,

$$\lambda = \frac{m_0(1-c_r)(m+1)\dot{\delta}^{(-)^2}}{2\widehat{\dot{\delta}}_c}\left(\frac{c_r m_0(n+1)\dot{\delta}^{(-)^2}}{2k}\right)^{-\frac{m+1}{n+1}} \tag{37}$$

Combined with Eq. (15), it can be found that Eq. (37) is completely consistent with Eq. (36). As $m = n$, the simplified expression of Eq. (36) is the same as the Eq. (42) in literature [19].

2.4. Simulations of the system dynamic equation and the approximate dynamic equation

For the exploration of the approximate dynamic equation deviations from the system dynamic equation, a series of numerical examples is conducted. As described above, by introducing equivalent indentation and equivalent velocities, the approximate dynamic equation for the system dynamic equation is proposed based on the rule of energy equivalence. Substituting Eq. (35) into Eq. (28), the expression for the approximate dynamic equation can be described as:

$$\begin{cases} m_0\ddot{\delta} + \left(\frac{k(m+1)}{n+1}\left(\frac{c_r m_0(n+1)\dot{\delta}^{(-)^2}}{2k}\right)^{\frac{n-m}{n+1}} + \lambda\frac{2\dot{\delta}^{(-)}}{3}\right)\delta^m = 0 \ \text{Compression phase} \\ m_0\ddot{\delta} + \left(\frac{k(m+1)}{n+1}\left(\frac{c_r m_0(n+1)\dot{\delta}^{(-)^2}}{2k}\right)^{\frac{n-m}{n+1}} - \lambda\frac{2c_r\dot{\delta}^{(-)}}{3}\right)\delta^m = 0 \ \text{Restitution phase} \end{cases} \tag{38}$$

The numerical examples are conducted based on the system dynamic Eq. (4) and the approximate dynamic Eq. (6). The relevant parameters (k, n, m, c_r, m_0, $\dot{\delta}^{(-)}$, λ and the time step) should be given out before the simulation. These parameters can be determined by experiment (c_r, m_0, $\dot{\delta}^{(-)}$), contact force models (m and λ) or relevant contact mechanics theory (k and n). The relevant parameters in this section were set as follows: k equals 2.41E11pa·m$^{1/2}$, n equals 1.5, $\dot{\delta}^{(-)}$ equals 2.8 m/s, m_0 equals 0.1 kg, the time steps are set to 1E-8 s, the values of the restitution coefficient c_r are set to 0.2, 0.5 and 0.8, and according to previous studies [7,14,19–24,26–37], the values of the damping term exponent m are set to 2.0, 1.5, 1.0, 0.65, 0.5 and 0.25. The values of hysteresis damping factor λ are calculated through Eq. (36). The four-order-Runge-Kutta method is applied to solve Eqs. (4) and (38).

The simulation results are illustrated in Figs. 3–8. The numerical results from the system dynamic Eq. (4) are deemed accurate, and the results from the approximate dynamic Eq. (38) are deemed approximate.

It can be seen that the approximate dynamic equation achieves a good approximation of the system dynamic equation, and it reveals that it is feasible to derive the hysteresis damping factor based on the system dynamic equation and the relationship between deformation velocity $\dot{\delta}$ and indentation depth δ, which is derived from the approximate dynamic equation. From Figs. 3–8, it can be seen that when m equals 1.5, simulation results are among the best. From the analysis of the approx-

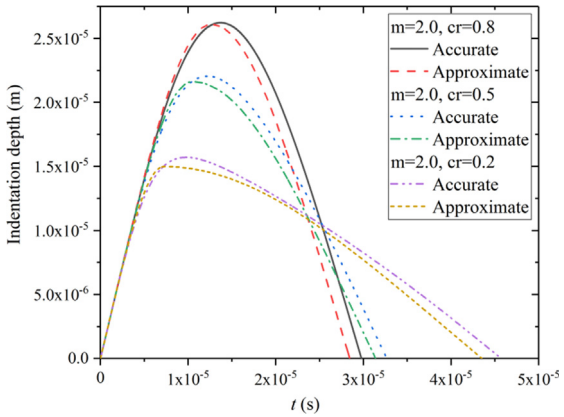

Fig. 3. Simulation results of the system dynamic equation and the approximate dynamic equation with m = 2.0.

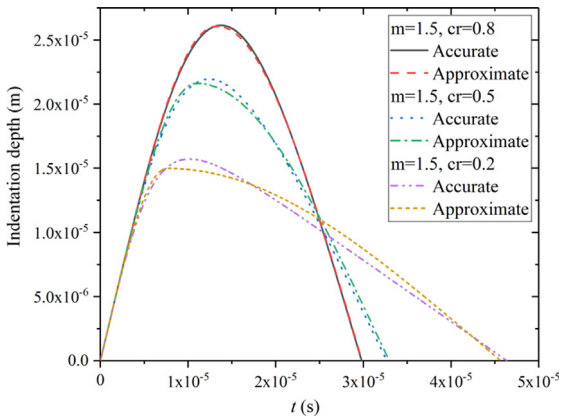

Fig. 4. Simulation results of the system dynamic equation and the approximate dynamic equation with m = 1.5.

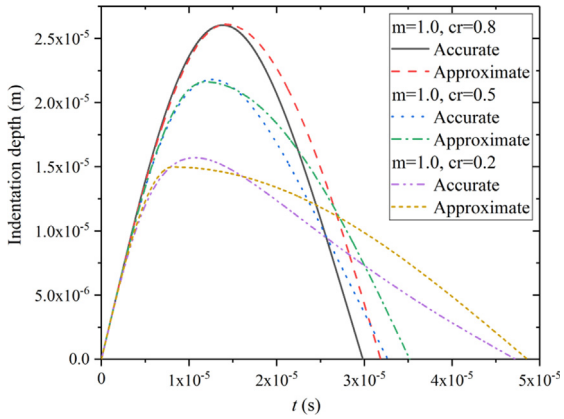

Fig. 5. Simulation results of the system dynamic equation and the approximate dynamic equation with m = 1.0.

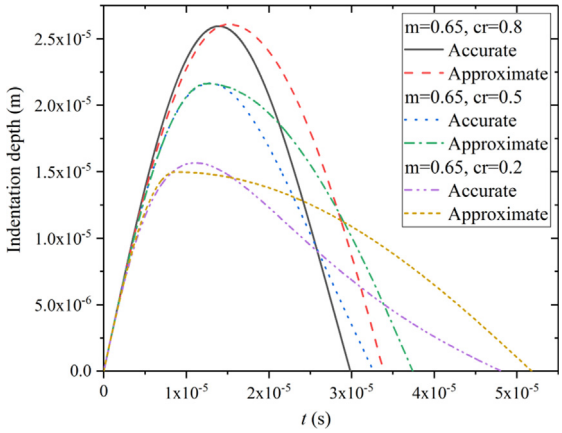

Fig. 6. Simulation results of the system dynamic equation and the approximate dynamic equation with m = 0.65.

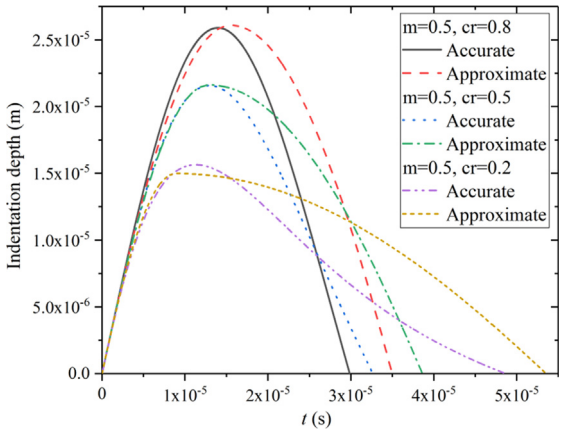

Fig. 7. Simulation results of the system dynamic equation and the approximate dynamic equation with m = 0.5.

imate contact force Eq. (7), it can be seen that when both m and n are equal to 1.5, the approximate term $k\widehat{\delta}^{n-m}\delta^{m}$ in Eq. (7) is strictly equal to the elastic force term $k\delta^{n}$ of the continuous contact force model, this may explain why the best simulation results are obtained when m = 1.5.

It can also be seen that the approximate dynamic equation does not perfectly match the system dynamic equation. The greater the difference between the value of m and 1.5, the greater the difference between the simulation results based on Eqs. (4) and (38). This is because when n equals 1.5, the greater the difference between the value of m and 1.5, the greater

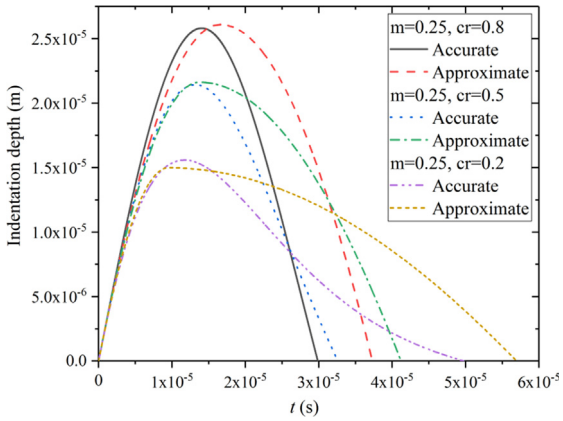

Fig. 8. Simulation results of the system dynamic equation and the approximate dynamic equation with m = 0.25.

the deviation between the approximate term $k\widehat{\delta}^{n-m}\delta^m$ in Eq. (7) and the elastic force term $k\delta^n$ in Eq. (1). The simulation results in Figs. 3 and 5–8 also show that obvious differences exist for the duration time. The results analysis reveals that the maximum relative error of maximum indentation is 3.85% but the maximum relative error of duration time is 26.38%. This occurs when m equals 0.25 and c_r equals 0.2. As described in Section 2.2, the approximate dynamic equation is proposed based on the rule of energy equivalence in the period from 0 to δ_{max} and from δ_{max} to 0. The duration time is not involved in the derivation of the approximate dynamic equation, this is likely to result in obvious differences in duration time. It can also be seen that the simulation results based on the approximate dynamic equation are closer to those based on the system dynamic equation in the compression phase than in the restitution phase. This should be related to the relatively longer duration of the restitution phase, but the exact reasons for this remain to be explored.

2.5. Establishing the new models via modification

Considering the deviation in the description of the system dynamic behavior between the approximate dynamic equation and the system dynamic equation, a more accurate model can be developed by modifying the primary formula of the hysteresis damping factor as illustrated in Eqs. (36) and (37). It can be seen from Eq. (37) that the analytical expression for the hysteresis damping factor contains the equivalent velocity $\widehat{\dot{\delta}}_c$, which is an approximate variable. Based on nondimensional analysis [33], the modification can be conducted by slightly adjusting the equivalent velocity.

The non-dimensional variables $x = \delta/\delta_{max}$ and $\tau = t/\left(\delta_{max}/\dot{\delta}^{(-)}\right)$ are introduced [33], it can be deduced that

$$\frac{d\delta}{dt} = \frac{d\delta}{dx}\cdot\frac{dx}{d\tau}\cdot\frac{d\tau}{dt} = \delta_{max}\frac{\dot{\delta}^{(-)}}{\delta_{max}}\frac{dx}{d\tau} = \dot{\delta}^{(-)}\frac{dx}{d\tau} \tag{39}$$

$$\frac{d^2\delta}{dt^2} = \frac{d\left(\frac{d\delta}{dt}\right)}{dt} = \frac{d\left(\dot{\delta}^{(-)}\frac{dx}{d\tau}\right)}{d\tau}\cdot\frac{d\tau}{dt} = \frac{\left(\dot{\delta}^{(-)}\right)^2}{\delta_{max}}\frac{d^2x}{d\tau^2} \tag{40}$$

Substituting $x = \delta/\delta_{max}$ and Eqs. (39) and (40) into Eq. (6) produces the dimensionless form of the system dynamic equation:

$$\frac{m_0\left(\dot{\delta}^{(-)}\right)^2}{\delta_{max}}\ddot{x} + k\delta_{max}^n x^n + \lambda\delta_{max}^m x^m\dot{\delta}^{(-)}\dot{x} = 0 \tag{41}$$

By denoting $k^* = \frac{k\delta_{max}^{n+1}}{m_0\left(\dot{\delta}^{(-)}\right)^2}$ and $\lambda^* = \frac{\lambda\delta_{max}^{m+1}}{m_0\dot{\delta}^{(-)}}$, Eq. (41) can be rewritten as the following form:

$$\ddot{x} + k^*x^n + \lambda^*x^m\dot{x} = 0 \tag{42}$$

Substituting Eqs. (35) and (37) into $k^* = \frac{k\delta_{max}^{n+1}}{m_0\left(\dot{\delta}^{(-)}\right)^2}$ and $\lambda^* = \frac{\lambda\delta_{max}^{m+1}}{m_0\dot{\delta}^{(-)}}$, it can be deduced that,

$$k^* = \frac{c_r(n+1)}{2} \tag{43}$$

$$\lambda^* = \frac{(1-c_r)(m+1)\dot{\delta}^{(-)}}{2\hat{\dot{\delta}}_c} \tag{44}$$

Considering the deviation in the description of the system dynamic behavior between the approximate dynamic equation and the system dynamic equation, the description of the hysteresis damping factor can be modified by a minor reduction of the approximate variable $\hat{\dot{\delta}}_c$. By introducing a modification parameter α, Eq. (44) can be rewritten as,

$$\lambda^* = \frac{(1-c_r)(m+1)\dot{\delta}^{(-)}}{2\alpha\hat{\dot{\delta}}_c} \tag{45}$$

Substituting Eq. (15) into Eq. (45), we obtain

$$\lambda^* = \frac{3(1-c_r)(m+1)}{4\alpha} \tag{46}$$

It can be seen that the nondimensional parameters k^* and λ^* depend on the exponent n and m, the coefficient of restitution c_r, and the modification parameter α.

Block diagram of the modification is shown in Fig. 9. The initial and final values of $\dot{x}$ are denoted as $\dot{x}^{(-)}$ and $\dot{x}^{(+)}$, respectively. When the parameters n, m, c_r, $\alpha$and $\dot{x}^{(-)}$ are set, numerical simulations can be conducted based on the dimensionless form of the system dynamic Eq. (42).

In this paper, the set value of the restitution coefficient, which is provided before the simulation for calculating λ^*, is defined as the pre-restitution coefficient. Based on the simulation results, an numerical restitution coefficient can be calculated through dividing $\dot{x}^{(+)}$ by $\dot{x}^{(-)}$, the numerical restitution coefficient is defined as the post-restitution coefficient. Previous studies have shown that there is a deviation between the values of the pre-restitution coefficient and the post-restitution coefficient, which should theoretically be the same [2,7,26,27]. The smaller the deviation is, the higher the model accuracy, because this deviation represents the deviation of the numerical separating velocity from the actual separating velocity and the deviation of the output predicted by the model from the actual behavior of the system. Therefore, the consistency of the post- and pre-restitution coefficients is considered an important criterion for modifying the model [19,27]. On the basis of

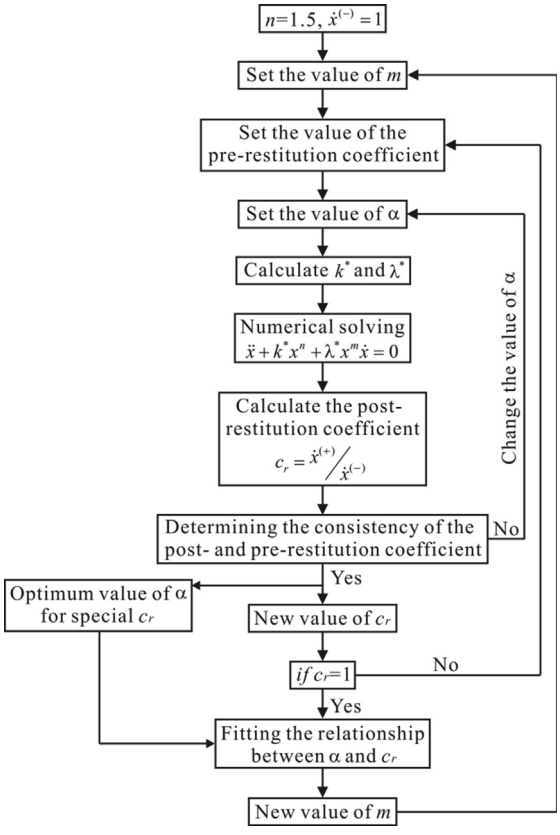

Fig. 9. Block diagram of the modification.

this criterion, the optimum values of the modification parameter α for different values of the restitution coefficient c_r can be obtained by a series of simulation experiments.

The expressions for the fitting function of the optimum values of the modification parameter α when n = 1.5 are as follows. According to previous studies [7,14,19–24,26–37], the exponent m is set to 2.0, 1.5, 1.0, 0.65, 0.5 and 0.25.

If m = 2.0,

$$\alpha = 1.363{c_r}^3 - 2.136{c_r}^2 + 0.8356c_r + 0.9404 \tag{47}$$

If m = 1.5 [19],

$$\alpha = 0.6181e^{-3.52c_r} + 0.899e^{0.09025c_r} \tag{48}$$

If m = 1.0,

$$\alpha = 1.514e^{-14.14c_r} + 1.289e^{-0.2474c_r} \tag{49}$$

If m = 0.65,

$$\alpha = 2.5891e^{-20.41c_r} + 1.417e^{-0.3188c_r} \tag{50}$$

If m = 0.5,

$$\alpha = 2.9191e^{-22.63c_r} + 1.468e^{-0.3505c_r} \tag{51}$$

If m = 0.25,

$$\alpha = 2.911e^{-23.87c_r} + 1.517e^{-0.356c_r} \tag{52}$$

The relationship between the post- and pre-restitution coefficients before and after the modification is illustrated in Fig. 10. It can be seen that after modification, the differences between the post- and pre-restitution coefficients are significantly reduced, which indicate that the model accuracy has been improved through the modification.

The modification method used above is also suitable for other value of m and n; therefore, a new type of continuous contact force model with an arbitrary damping term exponent m and arbitrary elastic term n is developed in this work.

By substituting the relevant formula of the modification parameter α into Eq. (36), the description of the modified hysteresis damping factor in the new type of continuous contact force model can be obtained

$$\lambda = \frac{3m_0(m+1)(1-c_r)\dot{\delta}^{(-)}}{4\alpha}\left(\frac{c_r m_0(n+1)\dot{\delta}^{(-)^2}}{2k}\right)^{-\frac{m+1}{n+1}} \tag{53}$$

The expression of contact force in the new model can be expressed as

$$F_c = k\delta^n + \frac{3m_0(m+1)(1-c_r)\dot{\delta}^{(-)}}{4\alpha}\left(\frac{c_r m_0(n+1)\dot{\delta}^{(-)^2}}{2k}\right)^{-\frac{m+1}{n+1}}\delta^m\dot{\delta} \tag{54}$$

Therefore, a new type of continuous contact force model is proposed in this research, in which the value of the elastic term exponent n and the damping term exponent m can be arbitrary.

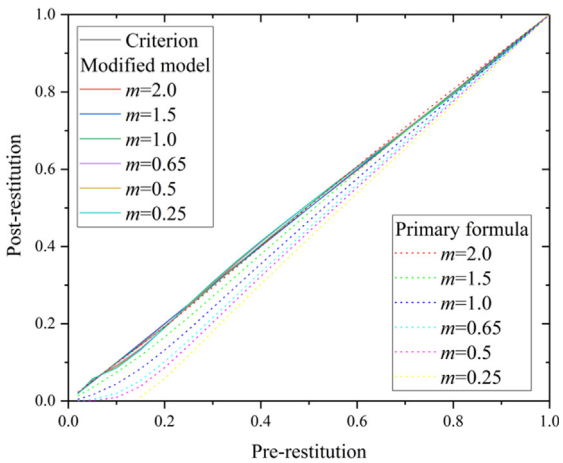

Fig. 10. Relation between the post- and pre-restitution coefficients before and after the modification.

3. Comparisons of the simulation and experimental results

The model proposed in Section 2 is constructed based on the consistency of the post- and pre-restitution coefficients and thus can provide a good simulation of the velocity changes before and after a collision and the system kinematics. We then further examine the performance of the models to obtain the description of the system dynamics. The change in velocity before and after the impact, the duration time and the peak contact force are the key description factors of impact modeling [19]. Experimentally investigating the model for the simulation accuracy of these three factors can validate the new models and evaluate the effect of different m-values on the accuracy of the continuous contact force model.

The experimental results published by Zhang and Sharf [49], which have been used in previous studies to compare several continuous contact force models [13,49], are utilized to validate and compare the contact models described in Section 3. A sketch of the experimental setup is shown in Fig. 11. A steel ball (mass m_0 = 0.54 kg) is released from the initial stationary position, and then a direct central normal impact occurs between the ball and the cylindrical specimen C2 with a preimpact velocity ranging from 0.0938 m/s $\leq v_0 \leq$ 0.5 m/s. The contact force and duration time are measured by an accelerometer, and the restitution coefficient is obtained by the dropweight tower experiment. The power exponent n = 1.5 and the stiffness coefficient k = 2.4144E10 N/L^n are given in [49].

Based on Eqs. (4) and (38), simulation experiments with different values of exponent m and preimpact velocity v_0 are conducted based on the four-order-Runge-Kutta method, and the time steps are set to 1E-8 s. The comparisons of the simulation and experimental results are listed in Table 3, and the relative errors between the simulation and experimental results are plotted in Fig. 12.

It can be seen that the new model constructed in this paper has reached a high accuracy with respect to the consistency of the post- and pre-restitution coefficients, duration time T and peak contact force F_{max}. The relative errors between the simulation and experimental results are less than 5%, which demonstrates the validity and potential of the new models. The effect of different m-values on the model accuracy can also be revealed by the comparison between the simulation and experimental results. As illustrated in Fig. 12, the relative errors on the consistency of the post- and pre-restitution coefficients are very low, less than 2%. The relative errors on the duration time are stable within approximately 4%, in most cases and variations in the value of m have little effect on the relative error. Relatively speaking, the peak contact force is most affected by the value of m. As seen in Table 3, the larger the m value is, the greater the calculated peak contact force. But it does not exist that the larger the m value is, the larger or smaller the absolute values of the relative errors on the peak contact force will be. Therefore, it can be found that there does not exist an optimal m value that minimizes the absolute values of the relative errors on the peak contact force.

Based on the above comparison and analysis, the validity and accuracy of the models constructed in this paper are tested, and it can also be seen that the value of m has little influence on the accuracy of the continuous contact force model, especially on the duration time and the consistency of the post- and pre-restitution coefficients. Moreover, there is no optimal value of m that maximizes the accuracy of the model. Therefore, the influence of the value of m on the model accuracy can be considered to be negligible.

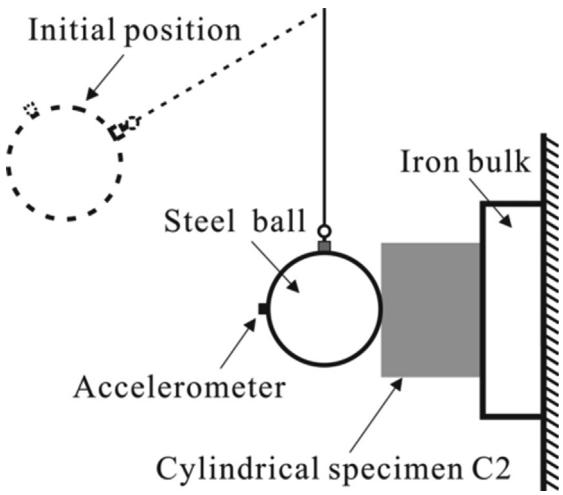

Fig. 11. The sketch of the experimental setup.

Table 3
Comparisons between the simulation and experimental data.

	Experiment results	Values of damping term exponent m					
		m = 2	m = 1.5	m = 1	m = 0.65	m = 0.5	m = 0.25
v_0 = 0.0938 m/s							
c_r	0.9166	0.9176	0.9166	0.9140	0.9126	0.9113	0.9105
T(10E-4 s)	2.76	2.8648	2.8648	2.8654	2.8655	2.8658	2.8658
F_{max} (N)	660.2	630.7	628.0	625.3	623.9	623. 1	622.3
v_0 = 0.1500 m/s							
cr	0.8892	0.8896	0.8892	0.8864	0.8848	0.8833	0.8822
T(10E-4 s)	2.52	2.6179	2.6175	2.6178	2.6178	2.6181	2.6180
F_{max} (N)	1076.6	1097.5	1089.9	1082.8	1078.9	1076.9	1074.8
v_0 = 0.2060 m/s							
c_r	0.8612	0.8608	0.8611	0.8586	0.8569	0.8551	0.8538
T(10E-4 s)	2.39	2.4674	2.4664	2.4663	2.4661	2.4663	2.4661
F_{max} (N)	1533.1	1594.3	1577.4	1562.7	1554.6	1550.8	1546.4
v_0 = 0.2989 m/s							
c_r	0.8234	0.8219	0.8232	0.8214	0.8197	0.8178	0.8162
T(10E-4 s)	2.23	2.3049	2.3031	2.3022	2.3016	2.3016	2.3011
F_{max} (N)	2447.9	2476.2	2435.3	2401.3	2382.4	2374.0	2363.8
v_0 = 0.3910 m/s							
c_r	0.7899	0.7877	0.7896	0.7887	0.7872	0.7852	0.7835
T(10E-4 s)	2.10	2.1980	2.1953	2.1935	2.1924	2.1923	2.1913
F_{max} (N)	3303.3	3409.5	3332.4	3269.4	3234.3	3219.4	3200.6
v_0 = 0.5000 m/s							
c_r	0.7568	0.7542	0.7564	0.7566	0.7555	0.7535	0.7517
T(10E-4 s)	2.0700	2.1068	2.1032	2.1003	2.0985	2.0981	2.0968
F_{max} (N)	4364.6	4581.1	4447.7	4338.4	4277.5	4252.7	4220.2

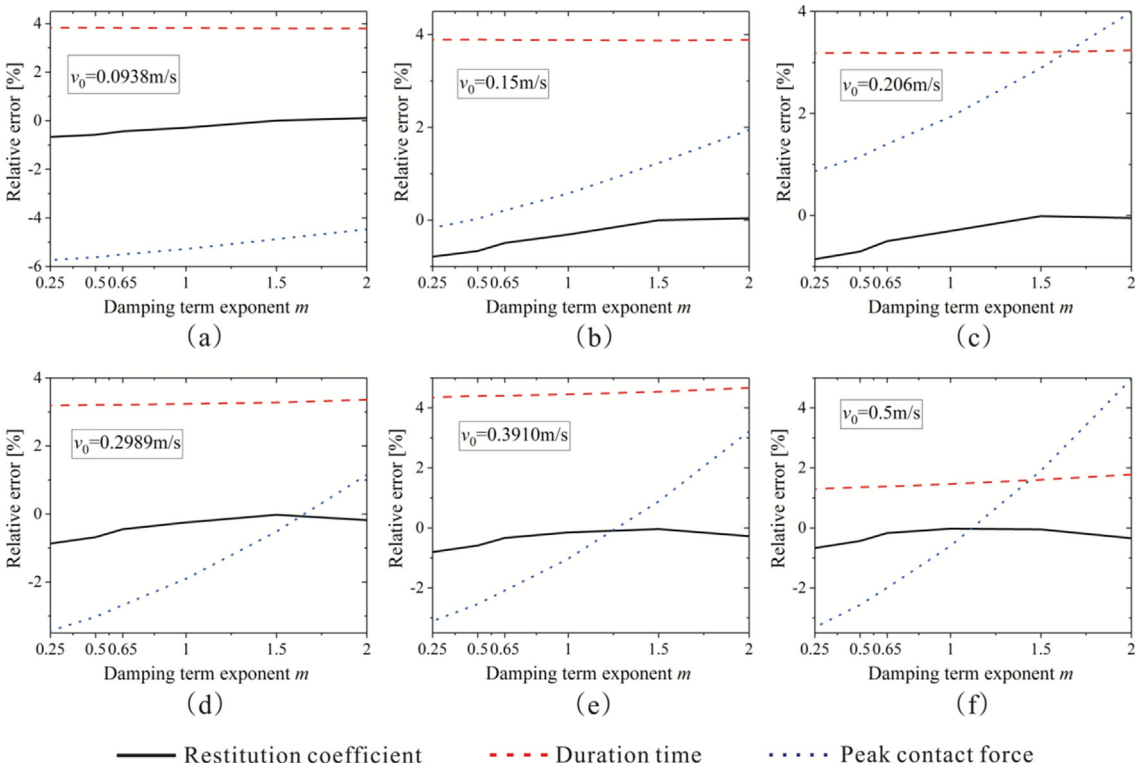

Fig. 12. Comparisons of the relative errors between the simulation and experimental data.

4. Conclusions

More than twenty continuous contact force models with several different values of damping term exponent have been presented for modeling contact-impact problems. How much does the value of damping term exponent affect the model accuracy? Is there an optimal value of damping term exponent that can provide the best model accuracy? To address these issues, this paper proposes a new type of continuous contact force model, in which the damping term exponent and elastic term exponent can be arbitrary. And the effect of the value of damping term exponent on the model accuracy is investigated based on the new model.

As it is almost impossible to obtain an analytical solution based on the system dynamic equation, based on the rule of energy equivalence, an approximate dynamic equation is developed by introducing the equivalent indentation and equivalent velocity. Then, a primary formula for the hysteresis damping factor of the model is derived based on the system dynamic equation and the approximate dynamic equation. The new model is constructed by modifying the primary formula through nondimensional analysis. The validities of the new model are demonstrated by the comparison between the simulation results and published experimental data. The comparison also reveals that the value of the damping term exponent has little influence on the accuracy of the model, especially on the duration time and the consistency of the post- and pre-restitution coefficients, and there is no optimal value of the damping term that maximizes the accuracy of the model.

CRediT authorship contribution statement

Jie Zhang: Methodology, Validation. **Huang Can:** Data curation, Validation. **Lei Zhao:** Visualization. **Di Jiejian:** Formal analysis, Writing - review & editing. **Guangping He:** Writing - review & editing. **Wenhao Li:** Supervision, Writing - review & editing.

Declaration of Competing Interest

The authors declare that they have no known competing financial interests or personal relationships that could have appeared to influence the work reported in this paper.

Acknowledgements

This research was supported by the National Natural Science Foundation of China [grant numbers 11702294, 12002002]; the National Key R&D Program of China under Grant No. 2019YFB1309603; the Joint Program of Beijing Municipal Foundation and Education Commission [grant number KZ202010009015]; and the Beijing Natural Science Foundation [grant number 3194047], and the Scientifific Research Foundation of North China University of Technology The author would like to thank to American Journal Experts for their English corrections.

References

[1] G. Gilardi, I. Sharf, Literature survey of contact dynamics modelling, Mech. Mach. Theory 37 (10) (2002) 1213–1239, https://doi.org/10.1016/s0094-114x(02)00045-9.
[2] S. Luka, S. Janko, B. Miha, A review of continuous contact-force models in multibody dynamics, Int. J. Mech. Sci. 145 (2018) 171–187, https://doi.org/10.1016/j.ijmecsci.2018.07.010.
[3] P. Flores, J. Ambrósio, J.C. Claro, H.M. Lankarani, Translational joints with clearance in rigid multibody systems, J. Comput. Nonlinear Dyn. 3 (1) (2008), https://doi.org/10.1115/1. 2802113 011007.
[4] Q. Tian, P. Flores, H.M. Lankarani, A comprehensive survey of the analytical, numerical and experimental methodologies for dynamics of multibody mechanical systems with clearance or imperfect joints, Mech. Mach. Theory 122 (2018) 1–57, https://doi.org/10.1016/j.mechmachtheory. 2017.12.002.
[5] A. Banerjee, A. Chanda, R. Das, Historical origin and recent development on normal directional impact models for rigid body contact simulation: a critical review, Arch. Comput. Method E. 24 (2) (2017) 397–422, https://doi.org/10.1007/s11831-016-9164-5.
[6] J. Ma, S. Dong, G. Chen, et al, A data-driven normal contact force model based on artificial neural network for complex contacting surfaces, Mech. Syst. Signal PR. (2021), https://doi.org/10.1016/j.ymssp.2021.107612.
[7] P. Flores, M. Machado, M.T. Silva, et al, On the continuous contact force models for soft materials in multibody dynamics, Multibody Syst. Dyn. 25 (3) (2011) 357–375, https://doi.org/10.1007/s11044-010-9237-4.
[8] K. Kardel, H. Ghaednia, A.L. Carrano, et al, Experimental and theoretical modeling of behavior of 3d-printed polymers under collision with a rigid rod, Addit. Manuf. 14 (2017) 87–94, https://doi.org/10.1016/j.addma. 2017.01.004.
[9] M. Anitescu, F.A. Potra, D.E. Stewart, Time-stepping for three-dimensional rigid body dynamics, Comput. Methods Appl. Math. 177 (3–4) (1999) 183–197, https://doi.org/10.1016/s0045-7825 (98)00380-6.
[10] P. Flores, R. Leine, C. Glocker, Modeling and analysis of planar rigid multibody systems with translational clearance joints based on the non-smooth dynamics approach, Multibody Syst. Dyn. 23 (2) (2010) 165–190, https://doi.org/10.1007/978-90-481-9971-6_6.
[11] J. Pang, D. Stewart, Differential variational inequalities, Math. Program. 113 (2) (2008) 345-424. https://doi.org/ 10.1007/s10107-006-0052-x.
[12] A. Tasora, D. Negrut, M. Anitescu, Large-scale parallel multi-body dynamics with frictional contact on the graphical processing unit, Proc. Inst. Mech. Eng., Proc., Part K, J. Multi-Body Dyn. 222 (4) (2008) 315–326, https://doi.org/10.1243/14644193jmbd154.
[13] J. Alves, N. Peixinho, M.T.D. Silva, et al, A comparative study of the viscoelastic constitutive models for frictionless contact interfaces in solids, Mech. Mach. Theory 85 (2015) 172–188, https://doi.org/10.1016/j.mechmachtheory.2014.11.020.
[14] H.M. Lankarani, P.E. Nikravesh, A contact force model with hysteresis damping for impact analysis of multibody systems, J. Mech. Des. 112 (3) (1990) 369–376, https://doi.org/10.1115/1.2912617.
[15] X. Zheng, F. Zhang, Q. Wang, Modeling and simulation of planar multibody systems with revolute clearance joints considering stiction based on an LCP method, Mech. Mach. Theory 130 (2018) 184–202, https://doi.org/10.1016/j.mechmachtheory.2018.08.017.

[16] R. Zhang, Y. Yu, Q. Wang, et al. An improved implicit method for mechanical systems with set-valued friction, Multibody Syst. Dyn. (2019) 1-28. https://doi.org/10.1007/s11044-019-09713- 0.
[17] M. Ezati, P. Brown, B. Ghannadi, et al, Comparison of direct collocation optimal control to trajectory optimization for parameter identification of an ellipsoidal foot-ground contact model, Multibody Syst. Dyn. 49 (2) (2020), https://doi.org/10.1007/s11044-020-09731-3.
[18] H. Hertz, Ueber die beruehrung fester elastischer koerper, J. Reine Angew. Math. 91 (1881) 156–171, https://doi.org/10.1515/crll.1882.92.156.
[19] J. Zhang, W. Li, L. Zhao, et al, A continuous contact force model for impact analysis in multibody dynamics, Mech. Mach. Theory 153 (2020), https://doi.org/10.1016/j.mechmachtheory.2020.103946 103946.
[20] K.H. Hunt, F.R.E. Crossley, Coefficient of restitution interpreted as damping in vibroimpact, J. Appl. Mech. 42 (2) (1975) 440–445, https://doi.org/10.1115/1.3423596.
[21] Y. Gonthier, J. McPhee, C. Lange, et al. A regularized contact model with asymmetric damping and dwell-time dependent friction, Multibody Syst. Dyn. 11 (3) 2004 209-233. https://doi.org/10.1023/B:MUBO.0000029392. 21648.bc.
[22] Y. Zhang, I. Sharf, Compliant force modeling for impact analysis, Proceedings of the 2004 ASME International Design Technical Conference, Salt Lake City, UT. https://doi.org/10.1115/DETC2004-57220.
[23] D.W. Marhefka, D.E. Orin, A compliant contact model with nonlinear damping for simulation of robotic systems, IEEE Trans, Syst. Man Cybern. Syst. Hum. 29 (1999) 566–572, https://doi.org/10.1109/3468.798060.
[24] Q. Zhiying, L. Qishao, Analysis of impact process based on restitution coefficient, J. Dyn. Control 4 (2006) 294–298.
[25] M. Gharib, Y. Hurmuzlu, A new contact force model for low coefficient of restitution impact, J. Appl. Mech.-T. Asme. 79 (6) (2012) 4506, https://doi.org/10.1115/1.4006494.
[26] S. Hu, X. Guo, A dissipative contact force model for impact analysis in multibody dynamics, Multibody Syst. Dyn. 35 (2) (2015) 131–151, https://doi.org/10.1007/s11044-015-9453-z.
[27] Y. Shen, D. Xiang, X. Wang, et al, A contact force model considering constant external forces for impact analysis in multibody dynamics, Multibody Syst. Dyn. 44 (4) (2018) 397–419, https://doi.org/10.1007/s11044-018-09638-0.
[28] R.G. Herbert, D.C. McWhannell, Shape and frequency composition of pulses from an impact pair, J. Eng. Ind. 99 (1977) 513–518, https://doi.org/10.1115/1.3439270.
[29] J. Lee, H.J. Herrmann, Angle of repose and angle of marginal stability: molecular dynamics of granular particles, J. Phys. A: Math. Gen. 26 (2) (1993) 373.
[30] G.H. Ristow, Simulating granular flow with molecular dynamics, J. Phys. I Fr. 2 (1992) 649–662, https://doi.org/10.1051/jp1:1992159.
[31] R. Jankowski, Analytical expression between the impact damping ratio and the coefficient of restitution in the non-linear viscoelastic model of structural pounding, Earthq. Eng. Struct. Dyn. 35 (4) (2006) 517-524. https:// doi.org/10.1002/eqe.537.
[32] M. Bordbar, T. Hyppänen, Modeling of binary collision between multisize viscoelastic spheres, J. Numer. Anal. Ind. Appl. Math. 2 (3–4) (2007) 115–128.
[33] G. Kuwabara, K. Kono, Restitution coefficient in a collision between two spheres, Jpn. J. Appl. Phys. 26 (8R) (1987) 1230, https://doi.org/10.1143/JJAP.26.1230.
[34] N.V. Brilliantov, F. Spahn, J.M. Hertzsch, et al, Model for collisions in granular gases, Phys. Rev. E. 53 (5) (1996) 5382–5392, https://doi.org/10.1103/physreve.53.5382.
[35] N.V. Brilliantov, F. Spahn, J.M. Hertzsch, et al, The collision of particles in granular systems, Phys. A. 231 (4) (1996) 417–424, https://doi.org/10.1016/0378-4371(96)00099-4.
[36] T. Schwager, T. Poschel, Coefficient of normal restitution of viscous particles and cooling rate of granular gases, Phys. Rev. E. 57 (1) (1998) 650–654, https://doi.org/10.1103/PhysRevE.57.650.
[37] Y. Tsuji, T. Tanaka, T. Ishida, Lagrangian numerical simulation of plug flow of cohesionless particles in a horizontal pipe, Powder Technol. 71 (3) (1992) 239–250, https://doi.org/10.1016/0032-5910(92)88030-L.
[38] S. Ken, Newton's cradle versus nonbinary collisions, Phys. Rev. Lett. 104 (12) (2010), https://doi.org/10.1103/physrevlett.104.124302 124302.
[39] J. Horabik, M. Beczek, R. Mazur, et al, Determination of the restitution coefficient of seeds and coefficients of visco-elastic Hertz contact models for DEM simulations, Biosyst. Eng. 161 (2017) 106–119, https://doi.org/10.1016/j.biosystemseng.2017.06.009.
[40] J. Sun, N. Lam, L. Zhang, et al, A note on Hunt and Crossley model with generalized visco-elastic damping, Int. J. Impact Eng. 121 (2018) 151–156, https://doi.org/10.1016/j.ijimpeng. 2018.07. 007.
[41] R. Jankowski, Non-linear viscoelastic modelling of earthquake-induced structural pounding, Earthq. Eng. Struct. D. 34 (6) (2005) 595–611, https://doi.org/10.1002/eqe.434.
[42] D. Cao, Y. Yang, H. Chen, et al, A novel contact force model for the impact analysis of structures with coating and its experimental verification, Mech. Syst. Signal PR. 70–71 (2016) 1056–1072, https://doi.org/10.1016/j.ymssp. 2015.08.016.
[43] J. Ma, G. Chen, L. Ji, et al, A general methodology to establish the contact force model for complex contacting surfaces, Mech. Syst. Signal PR. 140 (2020), https://doi.org/10.1016/j.ymssp.2020.106678 106678.
[44] G. Marcial, M.C. Alberto, A nonlocal contact formulation for confined granular systems, J. Mech. Phys. Solids 60 (2012) 333–350, https://doi.org/10.1016/j.jmps.2011.10.004.
[45] S. Sundar, J.T. Dreyer, R. Singh, Estimation of impact damping parameters for a cam–follower system based on measurements and analytical model, Mech. Syst. Signal PR. 81 (2016) 294–307, https://doi.org/10.1016/j.ymssp. 2016.02.033.
[46] V.L. Popov, Contact mechanics and friction, first ed., Springer, Berlin Heidelberg, Berlin, 2010.
[47] K.L. Johnson, Contact mechanics, first ed., Cambridge University Press, London, 1985.
[48] H.M. Lankarani, P.E. Nikravesh, Continuous contact force models for impact analysis in multibody systems, Nonlinear Dyn. 5 (1994) 193–207, https://doi.org/10.1007/BF00045676.
[49] Y. Zhang, I. Sharf, Validation of nonlinear viscoelastic contact force models for low speed impact, J. Appl. Mech.-T. Asme. 76 (5) (2009), https://doi.org/10.1115/1.3112739.